# Wide-View Vertical Field Switching Blue-Phase LCD

Hui-Chuan Cheng, Jin Yan, Takahiro Ishinabe, Ching-Huan Lin, Kang-Hung Liu, and Shin-Tson Wu, *Fellow, IEEE*

***Abstract*—We report three major approaches for improving the contrast ratio and viewing angle of a vertical field switching (VFS) blue-phase liquid crystal display (BPLCD). The first approach involves compensation films, the second one uses wire-grid polarizer, and the third one employs an E-type analyzer. Our simulation results show that a contrast ratio over 1000:1 can be achieved. For wide-view applications, we could use a diffuser or curved turning film to steer the high contrast images to different viewing angles.**

***Index Terms*—Blue phase liquid crystal (BPLC), vertical field switching (VFS), wide-viewing angle.**

## I. Introduction

POLYMER-STABILIZED blue-phase liquid crystal (PS-BPLC) [1]–[3] is emerging as next-generation display technology because of its fast gray-to-gray response time [4], [5], isotropic dark state, and no need for alignment layer. In particular, the fast response time of BPLC enables color sequential displays using RGB LEDs, which in turn eliminates the spatial color filters. Consequentially, the optical efficiency and resolution density are all tripled. The elimination of color filters and tripled optical efficiency will make BPLCD a greener technology, while the tripled resolution density is critically important for 3D and 4 K-by-2 K high resolution displays.

So far, most BPLC devices utilize in-plane switching (IPS) [6], [7] or protruded electrodes [8]–[11]. IPS BPLCD is simple and has wide view, but its operating voltage is high and hysteresis is fairly large because the lateral field is spatially nonuniform and the peak electric field near electrode edges is high [12]. Protruded electrodes lower the operation voltage, but the tradeoff is increased fabrication complexity. To overcome the fabrication problem, vertical field switching (VFS) has been proposed recently [13], [14]. With this novel VFS mode, the operating voltage is greatly reduced and hysteresis is completely suppressed. However, how to achieve wide view remains a challenge.

In this paper, we present three approaches for improving the contrast ratio (CR) and viewing angle of a VFS BPLCD. We also analyze the pros and cons of each approach.

Manuscript received May 17, 2012; revised June 26, 2012; accepted July 15, 2012. Date of publication September 07, 2012; date of current version November 19, 2012.

H.-C. Cheng, J. Yan, and S.-T. Wu are with the College of Optics and Photonics, University of Central Florida, Orlando, FL 32816 USA (e-mail: hccheng@creol.ucf.edu and swu@mail.ucf.edu).

T. Ishinabe is with the Department of Electronics, Graduate School of Engineering, Tohoku University, Sendai 980-8579, Japan. (e-mail: ishinabe@ecei.tohoku.ac.jp)

C.-H. Lin and K.-H. Liu are with AU Optronics, Hsinchu 30078, Taiwan (e-mail: ChinHaun.Lin@auo.com).

Color versions of one or more of the figures are available online at http://ieeexplore.ieee.org.

Digital Object Identifier 10.1109/JDT.2012.2209399

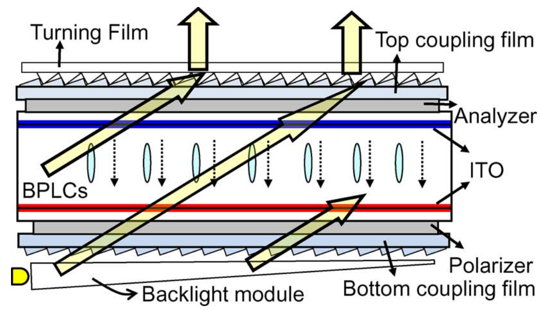


Fig. 1. Device structure of the proposed VFS BPLCD.

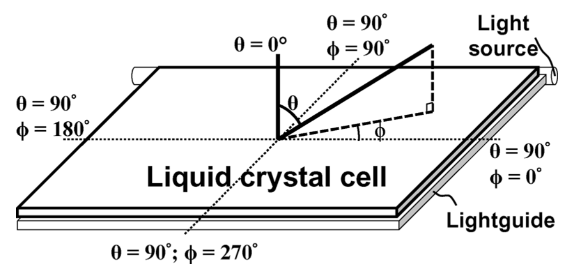


Fig. 2. Polar coordinate of VFS-BPLCD.

## II. Device Structure and Light Leakage

Fig. 1 depicts the structure of a VFS BPLCD [13], [14]. A directional backlight [15], [16] with oblique output is adopted. A larger incident angle results in a larger phase retardation which helps to lower the operating voltage. Typically, the directional backlight has a divergence angle (full width at half maximum FWHM) smaller than 20°. The bottom coupling film is designed to couple the oblique light into the BPLC cell and keep the light with a large incident angle. The top coupling film is to couple the oblique light out of the cell instead of being trapped by total internal reflection (TIR). A turning film is to steer the oblique light to the viewer's direction by TIR.

The polar coordinate in our device and simulation is defined in Fig. 2. Because the backlight passes the polarizer and analyzer obliquely ($\theta \sim 70°$, $\phi \sim 270°$), there is light leakage at the dark state if the polarizer and analyzer are set at $\phi = 45°$ and $-45°$ as a conventional LCD [17], [18]. To minimize light leakage, we can rotate the absorption axes of polarizer and analyzer along $\phi = 71.12°$ and $-71.12°$, respectively, as shown in Fig. 3(a), in which the polarizer and the analyzer are crossed at the backlight angle ($\theta = 70°$, $\phi = 270°$) as shown by Fig. 3(b).

We used commercial software, LCD Master (Shintech), and Nitto Denko's polarizer and analyzer (SEG1425DU) in our simulations. We assumed the BPLC composite is optically isotropic with $n_i = 1.55$ at $\lambda = 550$ nm at the voltage-off state. As the

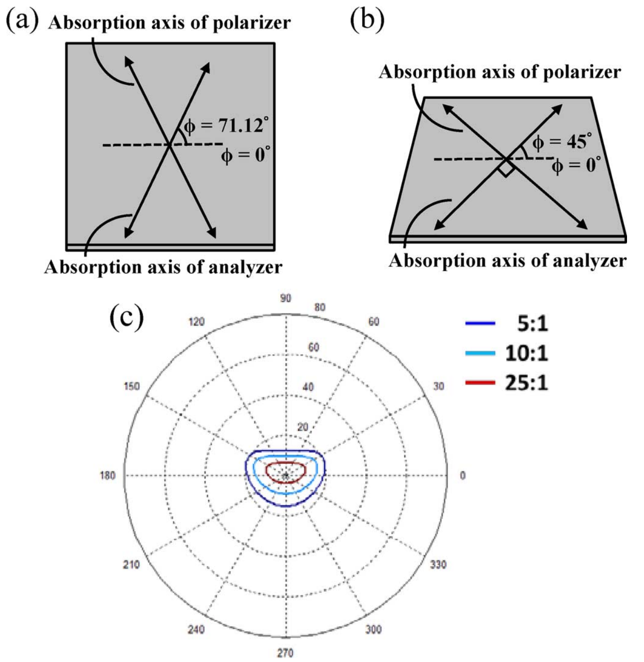


Fig. 3. Change in the effective angle between the polarizer and the analyzer: (a) normal observation ($\theta = 0°$); (b) oblique observation ($\theta = 70°$); and (c) simulated isocontrast contours.

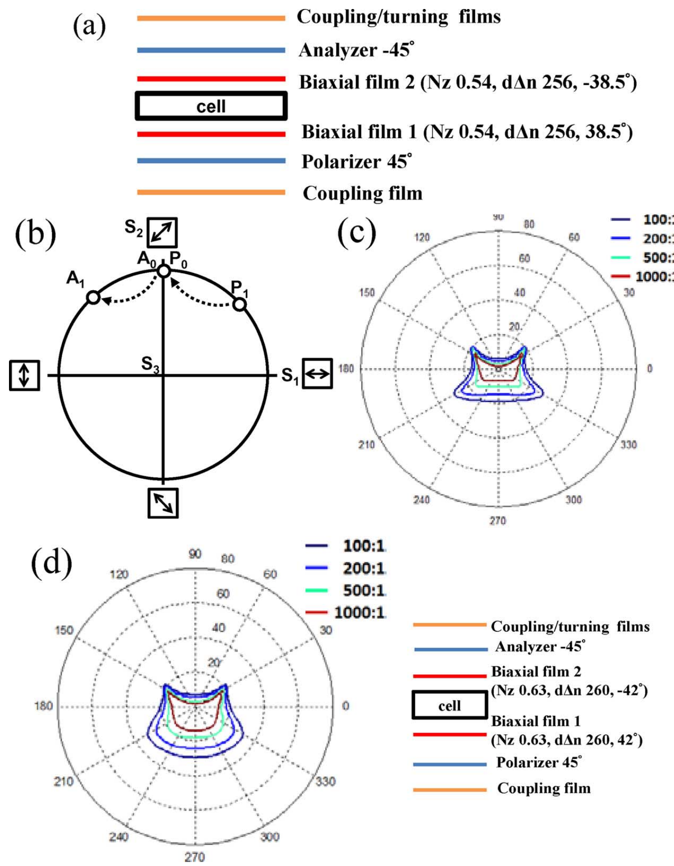


Fig. 4. Biaxial film-compensated VFS BPLCD: (a) device configuration, (b) compensation principle on Poincare sphere, and simulated isocontrast contours at incident angle $\theta = 70°$ (c) and $\theta = 60°$ (d). $\lambda = 550$ nm.

voltage increases, Kerr effect-induced birefringence $\Delta n$ gradually increases. When $\Delta n = 0.03$ and cell gap $= 4.74\ \mu$m, the phase retardation $\delta = \pi$ at 70° incident angle of our VFS cell. We can assume the induced $n_o \sim 1.54$ and $n_e \sim 1.57$ [19]. Fig. 3(c) shows the simulated isocontrast contours of Fig. 3(b) after the incident oblique backlight is steered to the normal direction by a turning film. Although the polarizer and analyzer are crossed at ($\theta = 70°$, $\phi = 270°$), the intrinsic CR is much lower than that of the crossed polarizers at normal incidence. Because the extinction ratio of the analyzer decreases drastically as the polar angle $\theta$ increases, in which the smaller effective absorption coefficient causes light leakage in the dark state. Therefore, how to enhance the intrinsic CR and widen the isocontrast contours becomes an urgent task for VFS BPLCD.

## III. Film Compensation Principle

As plotted in Fig. 3(c), the polarizer and analyzer at $\phi = 71.12°$ and $-71.12°$ leads to a fairly poor contrast ratio and narrow viewing angle. We could design retardation films to widen the isocontrast contours. However, the maximum CR (or the intrinsic CR) is not improved. On the other hand, we could reduce the azimuthal angle $\phi$ to enhance the effective absorption coefficient and improve the intrinsic CR. In this case, the polarizer and analyzer are not mutually perpendicular at the viewing angle of $\theta = 70°$ and $\phi = 270°$. It would be even harder to design the phase compensation films to widen the isocontrast contour for a small $\phi$. According to our experience, we should find a balance between high CR and wide isocontrast contour by choosing a proper $\phi$ between the polarizer and the analyzer.

Fig. 4(a) shows our first proposed optical configuration for VFS BPLCD. The absorption axes of polarizer and analyzer are along $\phi = 45°$ and $-45°$ respectively. Because the effective angles between polarizer and analyzer become 12.88° and $-12.88°$ rather than mutually perpendicular at oblique incident angle ($\theta = 70°$, $\phi = 270°$), the noticeable light leakage degrades the CR dramatically. We add two identical biaxial films set at $\phi = 38.5°$ and $-38.5°$ to reduce the light leakage. The $N_z$ factor, which is defined as $(n_x - n_z)/(n_x - n_y)$, is 0.54 for both biaxial films, and $d(n_x - n_y) = 256$ nm, here $d$ is the biaxial film thickness.

Fig. 4(b) shows the compensation process for the dark state on the Poincaré sphere. At normal incidence, i.e., $\theta = 0°$, the polarization state after polarizer $P_0$ is the same as the absorption axis of analyzer $A_0$. However, the effective angle between the polarizer and the analyzer changes as the incident backlight tilts away from normal (e.g., $\theta = 70°$, $\phi = 270°$). Therefore, the transmittance state $P_1$ deviates from analyzer $A_1$ and the light leakage happens. We add two biaxial films to compensate the separation of $P_1$ from $A_1$. Biaxial film 1 shifts the polarization state from $P_1$ to $P_0$, and subsequently biaxial film 2 moves the polarization state from $P_0$ to $A_1$. As a result, light leakage is suppressed substantially. Fig. 4(c) shows the simulated CR and isocontrast contours optimized at incident angle ($\theta = 70°$, $\phi = 270°$) for $\lambda = 550$ nm. From Fig. 4(c), CR $> 1000:1$ covers $\sim 10°$ viewing cone which is sufficient for the employed directional backlight (FWHM $< 20°$) in our VFS BPLCD. In order to widen the viewing angle, a front diffuser [20] or a

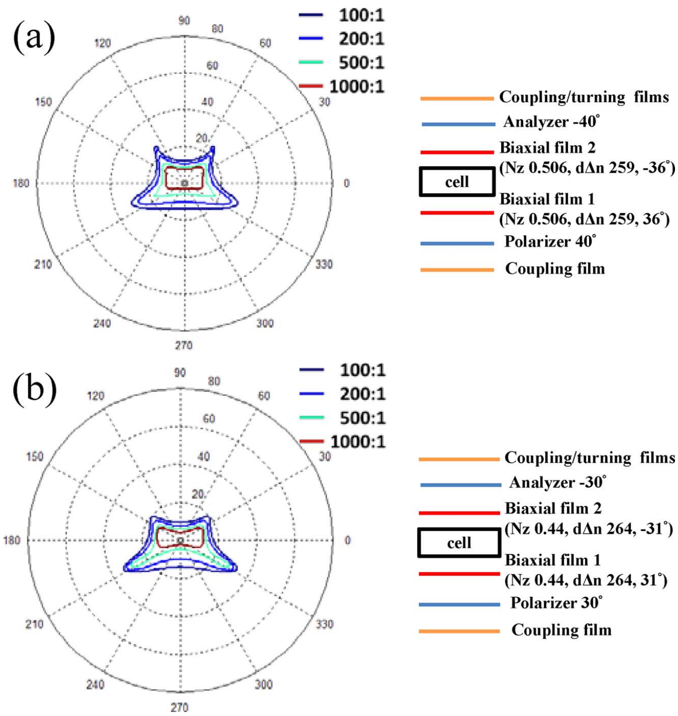


Fig. 5. Simulated isocontrast contours of biaxial film-compensated VFS BPLCD: (a) $\phi = 40°$ and $-40°$ and (b) $\phi = 30°$ and $-30°$.

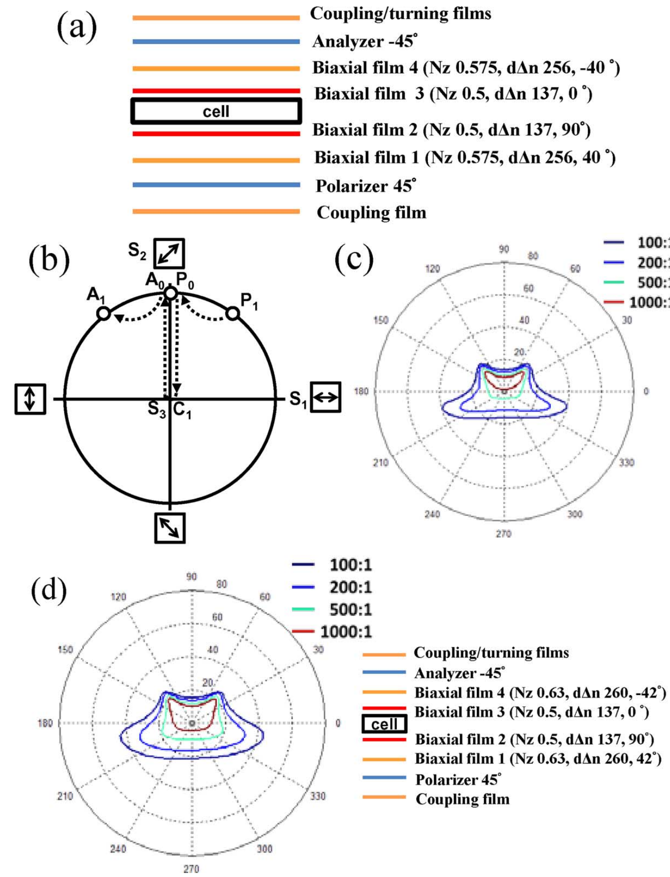


Fig. 6. Optical configuration of a VFS BPLCD with 4 biaxial films: (a) film configuration, (b) compensation principle, and simulated isocontrast contours at $\theta = 70°$ (c) and $\theta = 60°$ (d).

curve-shaped turning film [14] can be applied to spread the directional backlight to the observer for achieving wide view.

Fig. 4(d) shows the simulated isocontrast contours and optical configuration which is optimized for a smaller incident polar angle $\theta = 60°$, $\phi = 270°$. The polarizer and analyzer are still set at $\phi = 45°$ and $-45°$. Two identical biaxial films ($N_z = 0.63$, $d(n_x - n_y) = 260$ nm) are set at $\phi = 42°$ and $-42°$. Under a smaller polar angle $\theta$, Fig. 4(d) shows wider isocontrast contours as compared to Fig. 4(c). However, a smaller incident angle $\theta$ corresponds to a lower induced birefringence of a VFS BPLC which leads to a higher operating voltage. Recently, Merck reported a high Kerr-constant BPLC material [21]. If we use this material, we can choose a smaller incident angle to obtain $1\pi$ phase retardation. A smaller incident angle helps to enlarge the isocontrast contours.

Let us return to the backlight angle ($\theta = 70°$, $\phi = 270°$) but varying the polarizer/analyzer angle. Fig. 5(a) shows the isocontrast contours at a smaller angle ($\phi = 40°$ and $-40°$) between the polarizer and the analyzer. Two biaxial films ($N_z = 0.506$, $d(n_x - n_y) = 259$ nm) are set at $\phi = 36°$ and $-36°$. Fig. 5(b) shows the isocontrast contours when the polarizer and the analyzer are further reduced to $\phi = 30°$ and $-30°$. The incident angle of backlight is still at ($\theta = 70°$, $\phi = 270°$). Two biaxial films ($N_z = 0.44$, $d(n_x - n_y) = 264$ nm) are set at $\phi = 31°$ and $-31°$. Comparing Figs. 4(c), 5(a), and (b), we find the contour size for CR $= 1000 : 1$ is similar but the contour shape changes as the absorption angle $\phi$ between the polarizer and analyzer varies. For practical applications, we should also consider the output profile of the directional backlight in order to choose an appropriate $\phi$ and the matched contour shape.

Fig. 6(a) shows another example of four biaxial films. The polarizer and analyzer are set at $\phi = 45°$ and $-45°$. The biaxial films 1 and 4 ($N_z = 0.575$, $d(n_x - n_y) = 256$ nm) are set at $\phi = 40°$ and $-40°$. The biaxial films 2 and 3 ($N_z = 0.5$, $d(n_x - n_y) = 137$ nm) are set at $\phi = 90°$ and $\phi = 0°$, respectively. From the Poincaré sphere in Fig. 6(b), biaxial film 1 shifts the polarization state from $P_1$ to $P_0$. Biaxial film 2 shifts the linear polarization state $P_0$ to circular polarization $C_1$, and then biaxial film 3 changes the circular polarization $C_1$ back to linear $P_0$. Finally the biaxial film 4 rotates the transmission state $P_0$ to align with the absorption axis of analyzer $A_1$. Here, $P_0$ and $A_0$ are for the normal incident $\theta = 0°$. $P_1$ and $A_1$ deviate from $P_0$ and $A_0$ due to the oblique incidence ($\theta = 70°$, $\phi = 270°$) of the directional backlight.

Because the circularly polarized light $C_1$ is independent of the azimuthal angle $\phi$ in the BPLC material, it helps to improve the brightness state of the VFS BPLCD. Actually, we also tried to use one biaxial film to shift the polarization state from $P_1$ to $C_1$ directly and another biaxial film to shift the polarization state from $C_1$ to $A_1$. However, this simpler configuration is very sensitive to the polar angle $\theta$ and our results are not promising. Fig. 6(c) shows the isocontrast contours when the directional backlight is at ($\theta = 70°$, $\phi = 270°$). Fig. 6(d) shows the isocontrast contours optimized for the incident angle ($\theta = 60°$, $\phi = 270°$) of the directional backlight. The polarizer and the analyzer are set along $\phi = 45°$ and $-45°$. The biaxial films 1 and 4 ($N_z = 0.63$ and $d(n_x - n_y) = 260$ nm) are set at $\phi = 42°$ and $-42°$. The biaxial films 2 and 3 ($N_z = 0.5$ and

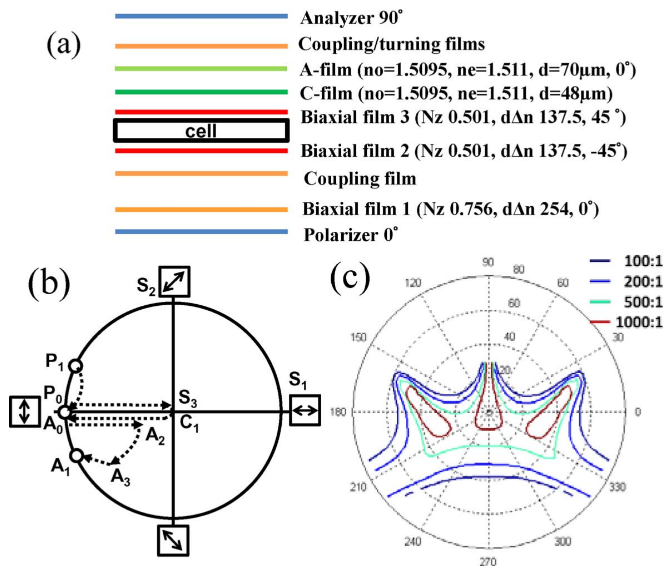


Fig. 7. Biaxial and A/C-films compensated VFS BPLCD: (a) film configuration, (b) compensation principle, and (c) simulated isocontrast contours.

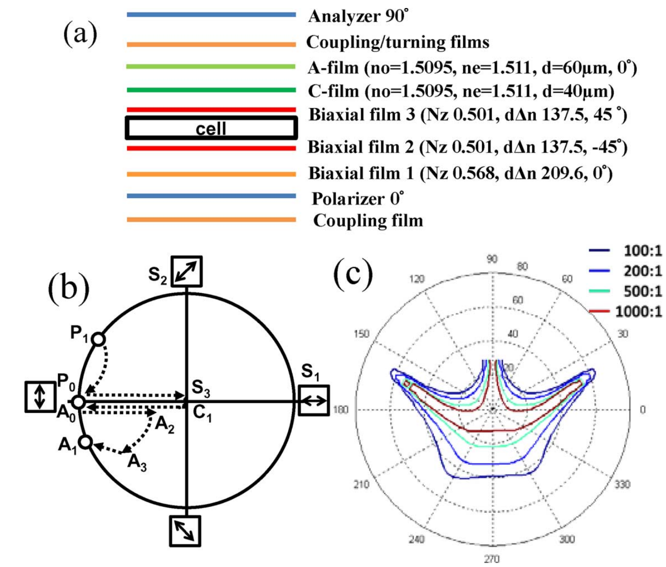


Fig. 8. Film-compensated VFS BPLCD with bottom coupling film laminated to the polarizer: (a) film configuration; (b) compensation principle; and (c) simulated isocontrast contours.

$d(n_x - n_y) = 137$ nm) are set at $\phi = 90°$ and $0°$, respectively. Fig. 6(d) exhibits wider isocontrast contours than Fig. 6(c) because of the smaller incident angle.

In all the above examples, the backlight passes the analyzer obliquely. If the coupling film and turning film are laminated between the analyzer and the BPLC cell, the light would pass the analyzer at normal angle and the analyzer would exhibit a good extinction ratio. Moreover, better image quality can be obtained if the coupling film and turning film are closer to the image plane (i.e., pixels of the LCD panel). Similarly, if we can place the polarizer outside the bottom coupling film [Fig. 7(a)], the directional backlight travels inside the polarizer at a smaller angle according to Snell's law. Hence, the extinction ratio of the polarizers and the device CR are all improved. A tradeoff is that the backlight might be depolarized by the turning films and the coupling film. As a result, we need additional retardation films to compensate for the depolarization effect.

Fig. 7(a) shows the schematic view of our approach. The polarizer and analyzer are at $\phi = 0°$ and $90°$, respectively. A biaxial film 1 ($N_z = 0.756, d(n_x - n_y) = 254$ nm) is set $\phi = 0°$. The biaxial films 2 and 3 ($N_z = 0.501, d(n_x - n_y) = 137.5$ nm) are set $\phi = -45°$ and $45°$. A C-film ($n_o = 1.5095$, $n_e = 1.511$, and thickness $d = 48$ $\mu$m) and an A-film ($n_o = 1.5095$, $n_e = 1.511$, thickness $\mathrm{d} = 70$ $\mu$m, and optical axis $\phi = 0°$) are laminated between the biaxial film 2 and the top coupling film. Fig. 7(b) shows the compensation process of the dark state on Poincaré sphere. For an oblique incidence ($\theta = 70°, \phi = 270°$), the transmission state $P_0$ is on the absorption axis of the analyzer $A_0$ and we get good dark state. However, when the azimuthal angle changes, such as $\phi = 315°$, the polarization state $P_1$ and the absorption axis $A_1$ deviates from $P_0$ and $A_0$. Biaxial film 1 does not change the polarization state $P_0$ at $\phi = 270°$ but can shift the polarization from $P_1$ to $P_0$ at $\phi = 315°$. Biaxial film 2 changes the linear polarization $P_0$ to circular $C_1$ and biaxial film 3 would change the circular light from $C_1$ to linear $P_0$. The C-film and A-film are designed to shift $P_0$ to $A_3$ via $A_2$. Finally, the top coupling film and turning film would depolarize the light $A_3$ and move $A_3$ to $A_1$; the absorption axis of the analyzer. Fig. 7(c) is a plot of the simulated isocontrast contours. The contours are improved noticeably because the polarizer and the analyzer exhibit larger extinction ratio at a small incident angle.

Fig. 8 shows another example by laminating bottom coupling film on the polarizer. The absorption axis of the polarizer and the analyzer are at $\phi = 0°$ and $90°$, respectively. Biaxial film 1 ($N_z = 0.568$, $d(n_x - n_y) = 209.6$ nm) is set at $\phi = 0°$. Identical biaxial films 2 and 3 ($N_z = 0.501$, $d(n_x - n_y) = 137.5$ nm) are set at $\phi = -45°$ and $45°$. A C-film ($n_o = 1.5095$, $n_e = 1.511$, and thickness $\mathrm{d} = 40$ $\mu$m) and an A-film ($n_o = 1.5095, n_e = 1.511$, thickness $\mathrm{d} = 60$ $\mu$m, and optical axis $\phi = 0°$) are laminated between the biaxial film 3 and the top coupling film. Fig. 8(b) shows the compensation process on Poincaré sphere for the dark state, which is the same as Fig. 7(b). Fig. 8(c) is a plot of the simulated isocontrast contours. Because the backlight's incident angle inside the polarizer is larger in Fig. 8 ($\theta \sim 70°$) than that in Fig. 7 ($\theta \sim 39°$), Fig. 8(c) shows smaller isocontrast contours than Fig. 7(c).

## IV. Wire-Grid Polarizer

We also explore the compensation method using wire-grid polarizers (WGPs) [22] instead of conventional dichroic sheet polarizer. Actually, WGP can substitute conventional polarizer in all above discussed examples. Because WGP retains a good extinction ratio at large incident angle (e.g., $\theta = 70°$), it helps to improve the CR. However, one shortcoming of WGP is that it reflects up to 50% of the ambient light which would degrade the CR. Thus, it is better to use WGP as the inner polarizer while keeping a sheet polarizer as the outer polarizer [23].

In Fig. 9(a), we show a special case by setting the absorption axis of a WGP at $\phi = 90°$ and a dichroic sheet analyzer at $\phi = 0°$. Usually, we do not set the dichroic polarizer at $\phi = 90°$ because of its poor extinction ratio at an oblique incidence

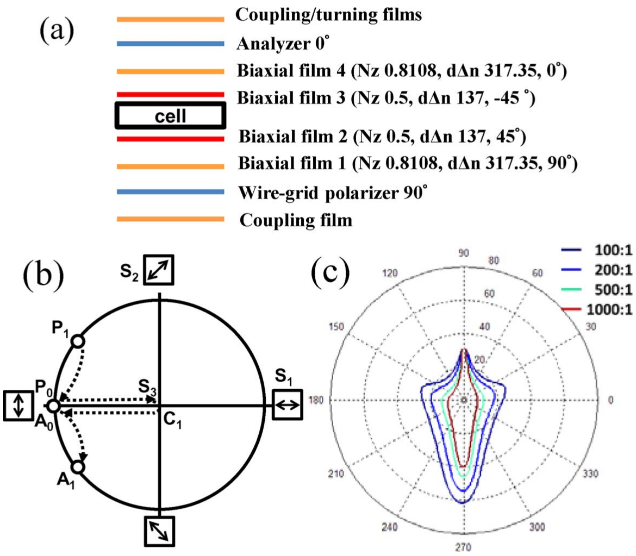


Fig. 9. Optical configuration of the proposed VFS-BPLCD, (a) film configuration, (b) compensation principle, and (c) simulated isocontrast contours.

($\theta = 70°$, $\phi = 270°$). The biaxial films 1 and 2 ($N_z = 0.81$, $d(n_x - n_y) = 317.35$ nm) are set at $\phi = 0°$ and 90°, and biaxial films 3 and 4 ($N_z = 0.5$ and $d(n_x - n_y) = 137$ nm) are at $\phi = 45°$ and $-45°$, respectively. Fig. 9(b) shows the compensation process of dark state by biaxial films on Poincaré sphere. When the oblique directional backlight ($\theta = 70°$, $\phi = 270°$) passes through WGP, it becomes linearly polarized $P_0$. Biaxial film 1 does not change the polarization state at $\phi = 270°$, but biaxial film 2 would shift the linear light from $P_0$ to circular $C_1$. Biaxial film 3 would shift the circular light from $C_1$ to linear which is parallel to the absorption axis of the analyzer $A_0$ and biaxial film 4 does not change the polarization state. Therefore, we can get a good dark state at ($\theta = 70°$, $\phi = 270°$). However, as the azimuthal incident angle changes (e.g., $\theta = 70°$, $\phi = 300°$), the polarization state $P_1$ deviates from $P_0$ and the absorption axis $A_1$ deviates from $A_0$. Biaxial film 1 can move $P_1$ back to $\mathrm{P}_0$ at different azimuthal angle (e.g., from $\phi = 225°$ to $\phi = 315°$). Next, biaxial films 2 and 3 shift the polarization state from $P_0$ to $P_2$ via $C_1$. Finally, biaxial film 4 reorients the linearly polarized light $P_2$ to be parallel to the absorption axis of the analyzer $A_1$. As a result, the light leakage is suppressed substantially. From the isocontrast contours shown in Fig. 9(c), the WGP is insensitive to the polar angle $\theta$ along $\phi = 90°/270°$ and provides wide isocontrast contours along its absorption axis. This special characteristic allows us to adopt 2D light-distribution backlight and front diffusor [24].

## V. E-Type Analyzer

The conventional LCDs adopt O-type analyzer in which ordinary ray is transmitted and extraordinary ray is strongly absorbed. For an O-type polarizer [Fig. 10(a)], the extinction ratio for E-wave attenuates gradually as the incident plane is parallel to the c-axis and the polar angle increases. While in Fig. 10(b), the E-type polarizer [25] can preserve a large extinction ratio for O-wave at different polar angles as the incident plane is perpendicular to the $c$-axis. Therefore, the polarization purity remains reasonably good at large incident angles for E-type polarizer.

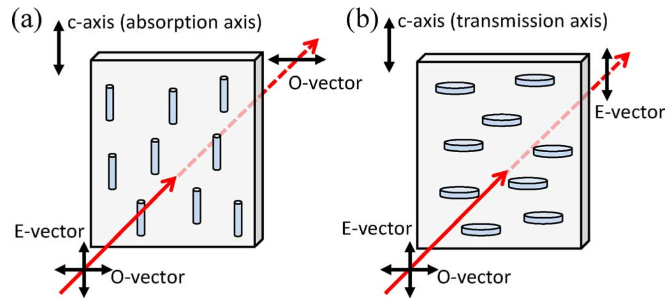


Fig. 10. Schematic drawing of an (a) O-type polarizer and (b) E-type polarizer.

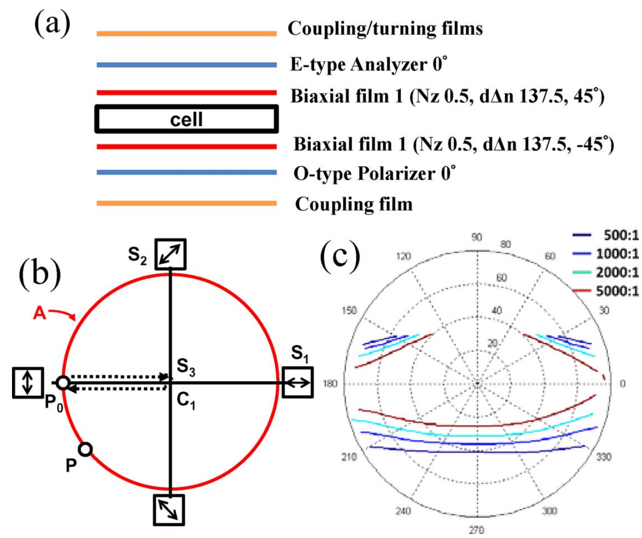


Fig. 11. Proposed VFS BPLCD using an O-type polarizer and an E-type analyzer: (a) film configuration; (b) compensation principle; and (c) simulated isocontrast contours.

Here, we propose a new design by using E-type analyzer instead of O-type for VFS BPLCD. As shown in Fig. 11(a), the absorption axis of a conventional O-type polarizer is along $\phi = 0°$. The c-axis (i.e., transmission axis) of an E-type analyzer is along $\phi = 0°$. Two biaxial films 1 and 2 ($N_z = 0.5$, $d(n_x - n_y) = 137.5$ nm) are set at $\phi = -45°$ and 45°.

Fig. 11(b) shows the compensation process on Poincaré sphere for achieving dark state. The polarization state is always at $P_0$ for different polar angles while the oblique backlight ($\phi = 270°$) passing through the polarizer. The transmitted light $P_0$ is polarized along the absorption axis of the E-type analyzer and a good dark state is obtained. For an E-type analyzer, all the light polarized perpendicular to the $c$-axis will be absorbed. Therefore, the absorption axis can be represented by the red circle in Fig. 11(b). For any incident light with azimuthal angle $\phi$ deviated from 270°, the transmitted state would shift from $P_0$ to another state, such as P, and is still on the red circle (i.e., absorption axis). Therefore, our configuration shows a good dark state which is insensitive to $\theta$ and $\phi$. No additional retardation film is needed to compensate the light leakage at dark state for different polar and azimuthal angles. In order to improve the bright state at different viewing angles, we add biaxial film 1 to shift the linear polarization $P_1$ to circular $C_1$. Biaxial film 2 shifts the circularly polarized light $C_1$ back to $A_1$; the absorption axis of analyzer. Fig. 11(c) shows the

TABLE I
COMPARISON OF DIFFERENT COMPENSATION METHODS.

| Methods | Contrast Ratio | Contour Range (V/H)* |
|---|---|---|
| without compensation | 10:1 | ±8°/±10° |
| 2 biaxial films | 1000:1 | ±8°/±10° |
| 5 retardation films | 1000:1 | ±20°/±40° |
| WGP + 4 biaxial films | 1000:1 | ±30°/±10° |
| E-type analyzer + 2 biaxial films | 5000:1 | ±30°/±90° |

*V/H: Vertical (ϕ=90°, 270°) / Horizontal (ϕ=0°, 180°)

simulated isocontrast contours optimized at incident angle ($\theta = 70°$, $\phi = 270°$). The E-type analyzer provides very wide isocontrast contours because it retains good extinction ratio for different $\theta$ and $\phi$.

## VI. DISCUSSION

We have proposed several device structures for improving the viewing angle of VFS BPLCD. With phase compensation films, we are able to enhance the intrinsic CR at normal direction and enlarge the isocontrast contours. Since VFS BPLCD uses a directional backlight ($\mathrm{FWHM} < 20°$), the high contrast contours should be larger than $\pm 10°$ viewing cone. If the oblique backlight is more collimated (e.g., $\mathrm{FWHM} < 10°$), we could choose the simplest configuration with two biaxial films. Otherwise, we need more retardation films to obtain wider isocontrast contours. The comparison of each compensation methods at incident angle $\theta = 70°$ is shown in Table I. Reducing the incident angle of a directional backlight can also enlarge the isocontrast contours. However, we need BPLC material with a higher Kerr-constant or we should apply a higher operating voltage. The E-type analyzer shows the best performance for VFS BPLCD. However, the E-type analyzer is presently not available commercially. To achieve wide view, a front diffusor or curved turning film can also be considered. The high contrast images are steered or diffused to different viewing angle. This kind of surface-diffusion LCD [20] helps to eliminate color shift and gray level inversion at different viewing angle.

## VII. CONCLUSION

The VFS BPLCD offers superior performances to IPS in operating voltage, transmittance, hysteresis, residual birefringence, and response time. Its cell structure is very simple, but it requires sophisticated phase compensation scheme to achieve wide view. Combined with the directional backlight and front diffuser, a $\mathrm{CR} > 1000:1$ can be achieved.

## REFERENCES


[1] H. Kikuchi, M. Yokota, Y. Hisakado, H. Yang, and T. Kajiyama, "Polymer-stabilized liquid crystal blue phases," *Nat. Mater.*, vol. 1, pp. 64–68, 2002.

[2] Y. Haseba, H. Kikuchi, T. Nagamura, and T. Kajiyama, "Large electro-optic Kerr effect in nanostructured chiral liquid-crystal composites over a wide temperature range," *Adv. Mater.*, vol. 17, p. 2311, 2005.

[3] J. Yan, L. Rao, M. Jiao, Y. Li, H. C. Cheng, and S. T. Wu, "Polymer-stabilized optically isotropic liquid crystals for next-generation display and photonic applications," *J. Mater. Chem.*, vol. 21, pp. 7870–7877, 2011.

[4] K. M. Chen, S. Gauza, H. Xianyu, and S. T. Wu, "Submillisecond gray-level response time of a polymer-stabilized liquid crystal," *J. Display Technol.*, vol. 6, no. 2, pp. 49–51, Feb. 2010.

[5] Y. Chen, J. Yan, J. Sun, S. T. Wu, X. Liang, S. H. Liu, P. J. Hsieh, K. L. Cheng, and J. W. Shiu, "A microsecond-response polymer-stabilized blue phase liquid crystal," *Appl. Phys. Lett.*, vol. 99, p. 201105, 2011.

[6] Z. Ge, S. Gauza, M. Jiao, H. Xianyu, and S. T. Wu, "Electro-optics of polymer-stabilized blue phase liquid crystal displays," *Appl. Phys. Lett.*, vol. 94, p. 101104, 2009.

[7] Z. Ge, L. Rao, S. Gauza, and S. T. Wu, "Modeling of blue phase liquid crystal displays," *J. Display Technol.*, vol. 5, pp. 250–256, Jul. 2009.

[8] L. Rao, Z. Ge, S. T. Wu, and S. H. Lee, "Low voltage blue-phase liquid crystal displays," *Appl. Phys. Lett.*, vol. 95, p. 231101, 2009.

[9] M. Kim, M. S. Kim, B. G. Kang, M. K. Kim, S. Yoon, S. H. Lee, Z. Ge, L. Rao, S. Gauza, and S. T. Wu, "Wall-shaped electrodes for reducing the operation voltage of polymer-stabilized blue phase liquid crystal displays," *J. Phys. D: Appl. Phys.*, vol. 42, p. 235502, 2009.

[10] Y. H. Kim, H. Lee, H. J. Park, O. J. Kwon, S. J. Yun, J. H. Park, S. Hong, and S. T. Shin, "The world's first blue phase liquid crystal display," in *SID Symp. Dig.*, 2011, vol. 42, pp. 122–125.

[11] M. Jiao, Y. Li, and S. T. Wu, "Low voltage and high transmittance blue-phase liquid crystal displays with corrugated electrodes," *Appl. Phys. Lett.*, vol. 96, p. 011102, 2010.

[12] L. Rao, J. Yan, S. T. Wu, Y. C. Lai, Y. H. Chiu, H. Y. Chen, C. C. Liang, C. M. Wu, P. J. Hsieh, S. H. Liu, and K. L. Cheng, "Critical field for a hysteresis-free BPLC device," *J. Display Technol.*, vol. 7, no. 12, pp. 627–629, Dec. 2011.

[13] H. C. Cheng, J. Yan, T. Ishinabe, and S. T. Wu, "Vertical field switching for blue-phase liquid crystal devices," *Appl. Phys. Lett.*, vol. 98, p. 261102, 2011.

[14] H. C. Cheng, J. Yan, T. Ishinabe, N. Sugiura, C. Y. Liu, T. H. Huang, C. Y. Tsai, C. H. Lin, and S. T. Wu, "Blue-phase liquid crystal displays with vertical field switching," *J. Display Technol.*, vol. 8, no. 2, pp. 98–103, Feb. 2012.

[15] M. Oe and I. Chiba, "Plane Light Source Unit," U.S. Patent 5 126 882, Jun. 30, 1992.

[16] K. Käläntär, "A monolithic segmented functional light guide for 2-D dimming LCD backlight," *J. Soc. Inf. Display*, vol. 19, pp. 37–47, 2011.

[17] X. Zhu, Z. Ge, and S. T. Wu, "Analytical solutions for uniaxial-film compensated wide-view liquid crystal displays," *J. Display Technol.*, vol. 2, no. 1, pp. 2–20, Mar. 2006.

[18] T. Ishinabe, T. Miyashita, and T. Uchida, "Wide-viewing-angle polarizer with a large wavelength range," *Jpn. J. Appl. Phys.*, vol. 41, pp. 4553–4558, 2002.

[19] J. Yan, M. Jiao, L. Rao, and S. T. Wu, "Direct measurement of electric-field-induced birefringence in a polymer-stabilized blue-phase liquid crystal composite," *Opt. Express*, vol. 18, pp. 11450–11455, 2010.

[20] K. Nakamura, T. Fuchida, K. Yamagata, A. Nishimura, T. Takita, and H. Takemoto, "Optical design of front diffuser for collimated backlight and front diffusing system," in *Proc. IDW*, 2011, pp. 475–477.

[21] M. Wittek, N. Tanaka, D. Wilkes, M. Bremer, D. Pauluth, M. K. Memmer, J. Canisius, A. Yeh, R. Yan, and K. Skjonnemand, "New materials for polymer-stabilized blue phase," in *SID Symp. Dig.*, 2012, vol. 43, pp. 25–28.

[22] S. W. Ahn, K. D. Lee, J. S. Kim, S. H. Kim, J. D. Park, S. H. Lee, and P. W. Yoon, "Fabrication of a 50 nm half-pitch wire grid polarizer using nanoimprint lithography," *Nanotechnol.*, vol. 16, pp. 1874–1877, 2005.

[23] Z. Ge and S. T. Wu, "Nanowire grid polarizer for energy efficient and wide-view liquid crystal displays," *Appl. Phys. Lett.*, vol. 93, p. 121104, 2008.

[24] M. Nishizawa, K. Kusama, K. Sekiya, B. Katagiri, T. Kawakami, and T. Uchida, "Investigation of novel diffuser films for 2D light-distribution control," in *Proc. IDW*, 2011, pp. 1385–1388.

[25] P. I. Lazarev and M. V. Paukshto, "Low-leakage off-angle in E-polarizers," *J. Soc. Inf. Display*, vol. 9, pp. 101–105, 2001.



**Hui-Chuan Cheng** received the B.S. degree in electrical engineering and M.S. degree in photonics from National Taiwan University, Taipei, Taiwan, in 2000 and 2005, respectively, and is currently working toward the Ph.D. degree in the College of Optics and Photonics, University of Central Florida (UCF), Orlando.

From 2005 to 2007, he was a senior engineer at AU Optronics, Hsinchu, Taiwan. His research interests include blue phase LCDs, sunlight readable LCDs, and touch panels.

Mr. Cheng is a recipient of 2011 and 2012 SID distinguished student paper awards. He was the president of SID student chapter at University of Central Florida (UCF), Orlando, in 2011.

**Jin Yan** is currently working toward the Ph.D. degree from the College of Optics and Photonics, University of Central Florida, Orlando.

Her research interest includes device physics and materials of polymer-stabilized blue phase and isotropic phase liquid crystal displays. She has 17 journal publications.

Currently, Ms. Yan is the president of SID student chapter at UCF. She is a co-recipient of 2012 SID distinguished student paper award.

**Takahiro Ishinabe** received the B.S., M.S., and Ph.D. degrees in electronic engineering from Tohoku University, Sendai, Japan, in 1995, 1997, and 2000, respectively.

From 2000 to 2002, he was a Research Fellow of the Japan Society for the Promotion of Science, and since 2003, he has been an Assistant Professor in the Department of Electronics, Graduate school of Engineering, Tohoku University, Sendai, Japan. He was a Visiting Professor at College of Optics and Photonics, University of Central Florida, from 2010 to 2011, researching on advanced liquid crystal displays.

Dr. Ishinabe is a recipient of the 2011 SID special recognition award. He is a senior member of SID.

**Ching-Huan Lin** received the B.S. and M.S. degrees in physics from National Cheng Kung University, Taiwan, in 1999 and 2001, respectively.

He has been a manager at AU Optronics, Hsinchu, Taiwan, since 2005. His current research interests include blue phase LCDs, transparent LCDs, and 3D displays.

Mr. Lin is a recipient of 2008 SID distinguished paper award. He received 37 U.S. patents and 5 Japan patents.

**Kang-Hung Liu,** photograph and biography not available at time of publication.

**Shin-Tson Wu** (M'98–SM'99–F'04) received the B.S. degree in physics from National Taiwan University, and the Ph.D. degree from the University of Southern California, Los Angeles.

He is a Pegasus professor at College of Optics and Photonics, University of Central Florida, Orlando.

Dr. Wu is the recipient of 2011 SID Slottow-Owaki prize, 2010 OSA Joseph Fraunhofer award, 2008 SPIE G. G. Stokes award, and 2008 SID Jan Rajchman prize. He was the founding Editor-in-Chief of IEEE/OSA JOURNAL OF DISPLAY TECHNOLOGY. He is a Fellow of the Society of Information Display (SID), Optical Society of America (OSA), and SPIE.